°C. The purple reaction mixture was warmed to room temperature and monitored by NMR spectroscopy. Within 2 h resonances for 4 had disappeared. No evidence was seen for the formation of $[(CpMo)(S_2CH_2)(S_2\overline{CH})MoCp]CF_3SO_3$.

Reaction of 1 with *n*-Butyl Isocyanide and Hydrogen in the Presence of Protic Acid. $CH_3(CH_2)_3NC$ (1.7 μL, 0.016 mmol) was added to a purple slurry of 1 (0.010 g, 0.016 mmol) and CF_3SO_3H (0.4 μL, 0.005 mmol) in 0.7 mL of degassed CD_2Cl_2 in an NMR tube. The reaction mixture was sealed under 450 Torr of hydrogen at −196 °C and warmed to room temperature. The reaction mixture was brown-purple after 10 min with much purple precipitate. A ^1H NMR spectrum showed resonances for 1 (35%), 4 (40%), and the unidentified complex also observed in the absence of hydrogen. Other broad resonances between 1.68 and 0.91 ppm were observed but were not resolved. Weak resonances for other molybdenum-containing products were also seen. After 3 h the resonances for 4 had nearly disappeared while the intensity of the Cp resonance for 1 increased somewhat relative to the methyl resonances of the isonitrile. Since 1 is only partially soluble in CD_2Cl_2, the relative intensity of its resonances does not accurately reflect its percentage in the two phase reaction mixture.

$[(CpMo)_2(\mu\text{-}S_2CH_2)(\mu\text{-}S)(\mu\text{-}SCCH_3{=}NH_2)](CF_3SO_3)_2$ (5). Triflic acid (15 μL, 0.16 mmol) was added to a purple solution of 1 (0.050 g, 0.081 mmol) in 10 mL of CH_3CN in a 100-mL Schlenk flask. No color change occurred as the solution was stirred at ambient temperature for 5 min. Addition of ~25 mL of diethyl ether gave a purple precipitate that was filtered, washed with ~10 mL of diethyl ether, and dried in vacuo; crude yield 0.035 g, 53%. ^1H NMR (CD_3CN): δ 7.19 (s, Cp), 4.38 (s, S_2CH_2), 2.45 (s, $CCH_3{=}NH_2$), 11.70 (br s, NH_2). FAB-MS: parent not observed, *m/e* 491 ($P^+ - NH_2$), 464 ($P^+ - CCH_3{=}NH_2$), 418 ($P^+ - SCH_2 - CCH_3{=}NH_2$). IR (KBr disk): 3105, 2926 (ν_{C-H} or ν_{N-H}), 1665 ($\nu_{C=N}$) cm^{-1}.

Reaction of Hydrogen with Benzylidenemethylamine in the Presence of 1. Complex 1 (0.010 g, 0.016 mmol) and $C_6H_5CH{=}NCH_3$ (2.0 μL, 0.016 mmol) were combined in 0.7 mL of CD_2Cl_2 in a NMR tube. The reaction mixture was sealed under 400 Torr of H_2 at −196 °C. The blue reaction mixture was warmed to ambient temperature and vigorously shaken. After 26 min, both $C_6H_5CH{=}NMe$ and $C_6H_5CH_2NHMe$ in equilibrium with their protonated forms were observed by proton NMR spectroscopy. After 1 day, greater than 95% conversion of $C_6H_5CH{=}NMe$ to $C_6H_5CH_2NHMe$ was observed.

Reaction of Hydrogen with Benzylidenemethylamine in the Presence of 1 and Protic Acid. Complex 1 (0.010 g, 0.016 mmol) and triflic acid (1.5 μL, 0.016 mmol) were combined in 0.7 mL of CD_2Cl_2 in a NMR tube. $C_6H_5CH{=}NMe$ (2 μL, 0.016 mmol) was added, and the purple reaction mixture was sealed under 400 Torr of H_2 at −196 °C. The reaction mixture was warmed to ambient temperature and vigorously shaken. The ^1H NMR spectrum after 2.5 h showed resonances consistent with $[C_6H_5CH{=}NHMe]^+$ and starting materials. On the basis of integration of C_6H_5 resonances, after 5 days ~67% of $[C_6H_5CH{=}NHMe]^+$ had been converted to $[C_6H_5CH_2NH_2Me]^+$. The concentration of 1 was unchanged throughout the reaction.

Reaction of 1 with Acetonitrile and Protic Acid in the Presence of Hydrogen. Complex 1 (0.05 g, 0.081 mmol) and triflic acid (7 μL, 0.077 mmol) were dissolved in 10 mL of acetonitrile and sealed under 400 Torr of H_2 at −196 °C. The purple-red reaction mixture was stirred 6 days at ambient temperature and turned light green after 4 days. Solvent was removed at reduced pressure, giving a green solid. ^1H NMR spectra of the crude solid in CD_3CN showed resonances for $(CpMo(\mu\text{-}S))_2S_2CH_2$ and $[(CpMo)(S_2CH_2)(S_2\overline{CCH_3})MoCp]^+$ in a 1:7.7 ratio based upon integration of Cp resonances. The solid was extracted with H_2O, and the H_2O was removed at reduced pressure, giving 0.015 g of a yellow solid. ^1H NMR spectra of the solid in D_2O showed resonances for acetamide and $[CH_3CH_2NH_3]CF_3SO_3$ in a 1.7:1 ratio based upon integration of methyl resonances. Acetamide appears to result from treatment of acetonitrile with aqueous acid.[5]

Acknowledgment. This work was supported by the National Science Foundation and, in part, by the National Institutes of Health.

Preparation, Molecular Structure, and Solution Properties of 1-[1,1′-Bis(diphenylphosphino)ferrocene]palladatetraborane

Catherine E. Housecroft,* Steven M. Owen, Paul R. Raithby, and Bilal A. M. Shaykh

University Chemical Laboratory, Lensfield Road, Cambridge CB2 1EW, U.K.

Received December 7, 1989

1-[1,1′-Bis(diphenylphosphino)ferrocene]palladatetraborane, 1-{(dppf)Pd}B_3H_7 (1), has been prepared by the reaction of (dppf)$PdCl_2$ with octahydrotriborate(1−). The molecular structure of 1 has been determined: triclinic, $P\bar{1}$ (No. 2), a = 9.557 (1), b = 9.632 (1), c = 18.547 (2) Å, α = 75.39 (1), β = 80.72 (1), γ = 73.41 (1)°, Z = 2, V = 1575.9 (5) Å^3, R_F = 0.025. The triborane ligand is symmetrically disposed (within esd's) with respect to the Pd atom; the central Pd–B distance is only slightly shorter (2.154 (3) Å) than the remaining two (2.190 (3) and 2.182 (3) Å). Borane hydrogen atoms have been located directly. Variable-temperature ^1H NMR spectroscopic studies indicate that two fluxional processes involving the {(dppf)Pd} fragment are operational; at $T \geq 203$ K, facile mutual twisting of the cyclopentadienyl rings occurs, while at $T \geq 293$ K, inversion at each phosphorus atom is accessed. The borane ligand itself appears to be static on the 400-MHz time scale, although inversion at the phosphorus atoms effectively renders equivalent the two distinct terminal hydrogen atoms on each terminal boron atom. Complex 1 shows an irreversible redox process, contrasting with reversible processes observed for dppf and (dppf)$PdCl_2$.

Recently we have been interested in a series of pseudo-square-planar complexes involving the coordination of palladium(II) to two phosphine donors and to a triborane(7) ligand.[1-4] The latter is formally $[B_3H_7]^{2-}$ and considered, in mononuclear complexes at least,[5] to be an analogue of a π-allyl moiety (viz, the borane is termed a π-borallyl ligand). Although a series of palladium(II) and platinum(II) π-borallyl complexes has been previously prepared and reported,[1,2] the structural characterization[2]

(1) Kane, A. R.; Muetterties, E. L. *J. Am. Chem. Soc.* **1971**, *93*, 1041.
(2) Guggenberger, L. J.; Kane, A. R.; Muetteries, E. L. *J. Am. Chem. Soc.* **1972**, *94*, 5665.
(3) Bould, J.; Greenwood, N. N.; Kennedy, J. D.; McDonald, W. S. *J. Chem. Soc., Dalton Trans.* **1985**, 1843.
(4) Greenwood, N. N.; Kennedy, J. D.; Reed, D. *J. Chem. Soc., Dalton Trans.* **1980**, 197.
(5) Housecroft, C. E.; Fehlner, T. P. *Inorg. Chem.* **1982**, *21*, 1739.

0276-7333/90/2309-1617$02.50/0

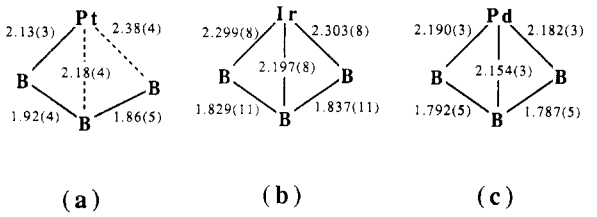

(a) (b) (c)

Figure 1. Comparison of the reported structural parameters for the MB_3 core of (a) $(Me_2PhP)_2PtB_3H_7$,[2] (b) $(OC)(Ph_3P)_2HIrB_3H_7$,[3] and (c) $(dppf)PdB_3H_7$, **1**.

of one member, $(Me_2PhP)_2PtB_3H_7$, suffered a severe orientational disorder and left an outstanding query as to whether the observed asymmetry of the $\{PtB_3H_7\}$ moiety (Figure 1a) was a real effect or not. Indeed, in $(OC)(Ph_3P)_2HIrB_3H_7$[3] the B_3H_7 unit is symmetrically disposed with respect to the metal atom (Figure 1b). A reinvestigation of pallada- and platinatetraborane complexes therefore seemed valuable, although we chose to extend the study to see to what extent changes in the electronic and/or steric properties of the phosphine ligands might influence the bonding mode and the reactivity of the coordinated borane. The 1,1′-bis(diphenylphosphino)ferrocene (dppf) chelate is a particularly attractive ligand since it is sterically quite demanding as indicated by a P–Pd–P bond angle in $(dppf)PdCl_2\cdot CHCl_3$[6] of 99.07 (5)° or in $(dppf)PdCl_2\cdot CH_2Cl_2$[7] of 97.98 (4)° compared with 85.82 (7)° in $(dppe)PdCl_2\cdot CH_2Cl_2$[8] (dppe = bis(diphenylphosphino)ethane). Furthermore, $(dppf)PdCl_2$ has been found to be a highly selective catalyst for cross-coupling in organic synthesis, and this property has been attributed to the large P–Pd–P bond angle enhancing the reductive elimination of the organopalladium intermediate.[6] The dppf ligand also provides a redox-active center that should be sensitive to the presence of (i) a Pd(II) center and (ii) the borane ligand.

Experimental Section

General Data. Manipulations were carried out under inert atmosphere using standard Schlenk techniques. Solvents were dried over suitable reagents, degassed, and distilled before use. $PdCl_2$ (Johnson-Matthey), dppf (Aldrich), and $[Me_4N][B_3H_8]$ (Alfa-Ventron) were used as received. Na_2PdCl_4 was prepared from NaCl and $PdCl_2$ by a method analogous to that described for the synthesis of $K_2Pd(CN)_4$.[9] FT NMR spectra were recorded on a Brüker AM 400 spectrometer. ^1H NMR chemical shifts are with respect to $\delta = 0$ for Me_4Si, ^{11}B NMR with respect to $\delta = 0$ for $F_3B\cdot OEt_2$, and ^{31}P NMR with respect to $\delta = 0$ for 85% H_3PO_4(aq). All downfield chemical shifts are positive. Infrared spectra were recorded on a Perkin-Elmer FT 1710 spectrophotometer. FAB mass spectra were recorded on a Kratos MS 890 instrument. Electrochemical measurements were made by the cyclic voltammetric method by using an Amel electrochemical system[10] (MeCN, $[^nBu_4N][BF_4]$ supporting electrolyte), Ag/AgCl reference electrode, double Pt bead, sweep rate = 20–200 mV s^{-1}, potentials referenced to internal Fc/Fc^+ added at the end of the experiment and quoted vs SCE fixed at −0.307 V vs Fc/Fc^+.

Preparation of $(dppf)PdCl_2$. The following method was used in preference to the literature procedure.[6] A solution of dppf (1.0 g, 1.8 mmol) in THF (30 mL) was added to a solution of Na_2PdCl_4 (0.53 g, 1.8 mmol) in ethanol (150 mL). A red precipitate of $(dppf)PdCl_2$ began to form immediately. After 1 h of stirring, solvent was removed by using a rotary evaporator, and the red product was washed with water (500 mL) and dried (80 °C, 12 h), yield of $(dppf)PdCl_2$ = 85%. Analytical data were as previously reported[6] and in addition: IR (KBr disk) ν_{PdCl} 310 w, 284 m cm^{-1}; FAB MS in 3-NBA matrix, m/z 732 (P^+).

Table I. Crystal Data for $(dppf)PdB_3H_7$, 1

formula	$C_{34}H_{35}B_3FeP_2Pd$
mol wt, M_r	699.6
cryst syst	triclinic
space group	$P\bar{1}$ (No. 2)
a, Å	9.557 (1)[a]
b, Å	9.632 (1)
c, Å	18.547 (2)
α, deg	75.39 (1)
β, deg	80.72 (1)
γ, deg	73.41 (1)
V, Å^3	1575.9 (5)
Z	2
D(calcd), g cm^{-3}	1.475
μ(Mo Kα), cm^{-1}	11.33
F(000)	712
T, K	290
radiation	Mo Kα (λ = 0.710 69 Å)
2θ limits, deg	$5.0 \le 2\theta \le 50.0$
data collected (h,k,l)	+11,±11,±22
no. of rflns coll	5918
no. of unique rflns	5423
no. of obs rflns ($F_o \le 4\sigma(F_o)$)	5100
R_F[b]	0.025
R_{wF}[c]	0.029
ω	$2.341/[\sigma^2(F) + 0.0005\lvert F^2\rvert]$

[a] Unit cell parameters obtained from least-squares fit of the angular settings of 25 reflections ($20 \le 2\theta \le 28°$). [b] $R_F = \sum(\lvert\lvert F_o\rvert - \lvert F_c\rvert\rvert)/\sum(F_o)$. [c] $R_{wF} = [\sum\omega(\lvert F_o\rvert - \lvert F_c\rvert)^2/\sum\omega(F_o)^2]^{1/2}$.

Preparation of 1-{(dppf)Pd}B_3H_7. $[Me_4N][B_3H_8]$ (0.12 g, 1.0 mmol) was added to a solution of $(dppf)PdCl_2$ (0.73 g, 1.0 mmol) in MeCN (100 mL), THF (50 mL), toluene (25 mL), and Et_3N (2.5 mL).[11] The mixture was stirred for 2 h and allowed to stand for 1 h as $[Me_4N]Cl$ precipitated. The supernatant was removed by cannula, solvent was removed in vacuo, and the solid residue was washed with methanol (50 mL). The product was separated by using column chromatography with Kieselgel 80 (70–230 mesh) and was eluted with hexane as the first band (yield ≈ 20%).[12] **1**: 400-MHz ^1H NMR (CD_2Cl_2, 203 K) δ 7.38–7.61 (20 H, *Ph*), 4.34 (2 H, *Cp*), P^+ (2 H, *Cp*), 4.14 (2 H, *Cp*), 3.82 (2 H, *Cp*), 2.88 and 2.57 (br, 5 H B*H*), −2.8 (br, 2 H, B*H*B); 128-MHz ^{11}B NMR (CD_2Cl_2, 293 K) δ +8.5 (m, 2 B, fwhm = 500 Hz, $^{11}B\{^1H\}$ fwhm = 400 Hz), +20.1 (m, 1 B, fwhm = 250 Hz, $^{11}B\{^1H\}$ fwhm = 200 Hz); 162-MHz ^{31}P NMR (CD_2Cl_2, 293 K) δ +12.50; IR (hexane, cm^{-1}) ν_{BH} 2498 s, 2421 s, 1890 m, 1543 m; FAB MS in 3-NBA matrix, m/z 701 (P^+), 661 ($P^+ - B_3H_7$), isotopic distribution matched that simulated for ($P^+ - B_3H_7$); pattern for P^+ complicated by overlapping envelopes due to hydrogen loss.

Crystal Structure Determination. Crystallographic data are collected in Table I. Suitable red-brown crystals were obtained by diffusion of Et_2O into a CH_2Cl_2 solution of **1** and were mounted in 0.5-mm thin-walled glass capillaries under nitrogen. Using a crystal with dimensions (0.30 mm × 0.42 mm × 0.52 mm, accurate cell dimensions, at room temperature, were obtained by least-squares refinement of 500 accurately centered reflections ($22 < 2\theta < 25°$) using a Stöe-Siemens four-circle diffractometer equipped with graphite-monochromated Mo radiation. Data collection was performed employing a 30-step ω/θ scan mode with a step width of 0.03° and step time in the range 0.5–2.0 s/step. No significant variation was observed in the three check reflections during data collection. An empirical absorption correction was

(6) Hayashi, T.; Konishi, M.; Kobori, Y.; Kumada, M.; Higuchi, T.; Hirotsu, K. *J. Am. Chem. Soc.* **1984**, *106*, 158.
(7) Butler, I. R.; Cullen, W. R.; Kim, T.-J.; Rettig, S. J.; Trotter, J. *Organometallics* **1985**, *4*, 972.
(8) Steffen, W. L.; Palenik, G. J. *Inorg. Chem.* **1976**, *15*, 2432.
(9) Bigelow, J. H. *Inorg. Synth.* **1946**, *2*, 245.
(10) Constable, E. C.; Ward, M. D. *J. Chem. Soc., Dalton Trans.*, in press.
(11) This solvent system is based upon that used in the synthesis of related bis(phosphino)pallada- and platinatetraborane complexes.[12]
(12) Other products of the reaction were identified by ^{11}B and ^1H NMR and mass spectroscopy as $Et_3N\cdot B_3H_7$, $Et_3N\cdot BH_3$, and $[Et_3NH]Cl$; the formation of $(dppf)(BH_3)_2$ was also confirmed by comparing spectroscopic data (^{11}B NMR δ −36.5, ^{31}P NMR δ +22.5) with those of an authentic sample prepared independently by the reaction dppf with $THF\cdot BH_3$.

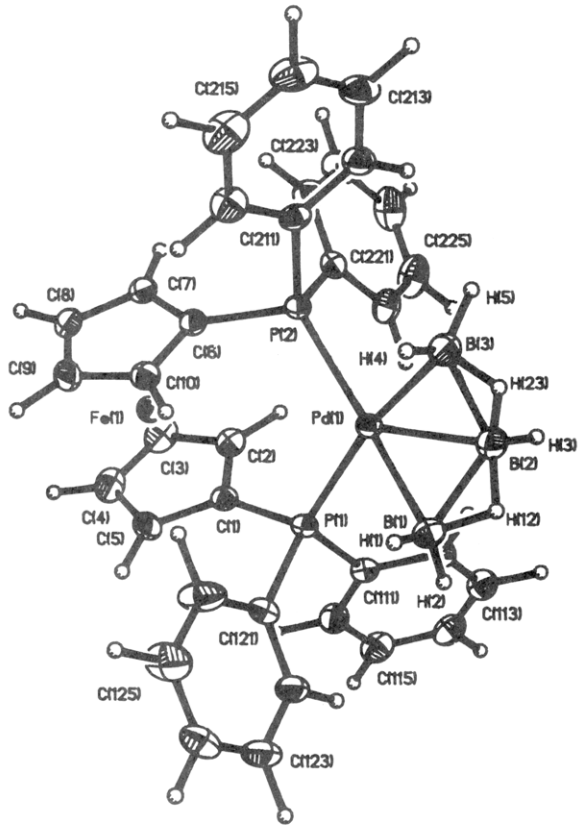

Figure 2. Molecular structure of (dppf)PdB_3H_7, 1.

applied to the data using 504 ψ-scan data from 14 reflections with $\psi > 70°$ (transmission factors 0.328 (max) and 0.268 (min)). The intensity data were converted to F_o after correction for Lorentz and polarization effects.

Structure Solution and Refinement. The possible space groups were $P1$ or $P\bar{1}$. The normalized structure factors suggested a centric distribution, and the centrosymmetric space group $P\bar{1}$ (No. 2) was confirmed by subsequent analysis. The positions of the Pd and Fe atoms were determined by a computer-assisted Patterson synthesis using SHELX86 (PATT).[13] The remaining non-hydrogen atoms were located from subsequent electron density difference syntheses. The structure was refined by blocked full-matrix least-squares analysis with all non-hydrogen atoms assigned anisotropic displacement parameters. Most of the H atoms were located from the electron density difference map and were introduced into the model. The H atoms coordinated to boron were refined freely with individual isotropic displacement parameters. Phenyl and cyclopentadienyl H atoms were placed in idealized positions (d(C–H) = 1.08 Å) and allowed to ride on the relevant C atom; each type of H was assigned a common isotropic displacement parameter. The weighting scheme (Table I) was introduced and gave satisfactory agreement analyses. The maximum shift/error in the final cycle of refinement was 0.07, and a difference electron density synthesis showed features only in the range +0.32 to −0.38 e Å^{-3}. The final R value is 0.025 for 5100 observed data ($F_o \geq 4\sigma(F_o)$) for 401 parameters. Atomic scattering factors for neutral atoms and anomalous dispersion corrections were taken from ref 14 (Pd, Fe) and SHELX76[15] (P, B, C, H). All calculations were performed using programs in refs 13, 14, or 16. Final atomic coordinates and equivalent isotropic displacement parameters are listed in Table II, and Figure 2 shows the atom numbering scheme used. Interatomic distances and angles are listed in Table III.

(13) Sheldrick, G. M. SHELX86, Program for Crystal Structure Solution: University of Göttingen: Göttingen, 1986.
(14) *International Tables for X-Ray Crystallography*; Kynoch Press; Birmingham, England, 1974; Vol. 4, pp 99–101, 149–150.
(15) Sheldrick, G. M. SHELX76, Program for Crystal Structure Determination: University of Cambridge, Cambridge, 1976.
(16) Motherwell, W. D. S.; Clegg, W. PLUTO, Program for Plotting Molecular and Crystal Structures; Universities of Cambridge and Göttingen, Cambridge and Göttingen, 1978.

Table II. Atomic Coordinates (×10^4) and Isotropic Thermal Parameters (Å^2 × 10^3) for 1

	x	y	z	U(eq)[a]
Pd(1)	1512 (1)	858 (1)	2748 (1)	30 (1)
Fe(1)	3700 (1)	−3137 (1)	2003 (1)	34 (1)
P(1)	1979 (1)	−1593 (1)	3482 (1)	31 (1)
P(2)	3006 (1)	637 (1)	1615 (1)	31 (1)
C(1)	3281 (3)	−3094 (2)	3109 (1)	34 (1)
C(2)	4769 (3)	−3081 (3)	2855 (1)	41 (1)
C(3)	5461 (3)	−4387 (3)	2576 (2)	56 (1)
C(4)	4411 (4)	−5213 (3)	2660 (2)	60 (1)
C(5)	3063 (3)	−4430 (3)	2990 (1)	48 (1)
C(6)	3203 (2)	−1081 (2)	1330 (1)	35 (1)
C(7)	4448 (3)	−2026 (3)	989 (1)	41 (1)
C(8)	4014 (3)	−3259 (3)	895 (1)	48 (1)
C(9)	2509 (3)	−3084 (3)	1164 (1)	46 (1)
C(10)	2014 (3)	−1745 (3)	1429 (1)	39 (1)
C(111)	2795 (2)	−1824 (3)	4348 (1)	35 (1)
C(112)	2961 (3)	−604 (3)	4562 (1)	42 (1)
C(113)	3606 (3)	−797 (3)	5210 (2)	50 (1)
C(114)	4105 (3)	−2186 (3)	5640 (1)	52 (1)
C(115)	3930 (3)	−3403 (3)	5441 (1)	55 (1)
C(116)	3285 (3)	−3229 (3)	4795 (1)	48 (1)
C(121)	347 (3)	−2316 (3)	3777 (1)	39 (1)
C(122)	−221 (3)	−2638 (3)	4512 (2)	55 (1)
C(123)	−1528 (4)	−3075 (4)	4684 (2)	70 (1)
C(124)	−2253 (3)	−3212 (3)	4146 (2)	63 (1)
C(125)	−1674 (4)	−2938 (5)	3416 (2)	80 (2)
C(126)	−393 (3)	−2469 (5)	3230 (2)	75 (2)
C(211)	2468 (3)	1993 (3)	746 (1)	37 (1)
C(212)	2801 (3)	3363 (3)	571 (1)	48 (1)
C(213)	2342 (3)	4409 (3)	−67 (2)	61 (1)
C(214)	1565 (4)	4093 (4)	−543 (2)	70 (1)
C(215)	1238 (4)	2731 (4)	−377 (2)	73 (1)
C(216)	1676 (3)	1691 (3)	271 (2)	54 (1)
C(221)	4871 (3)	745 (3)	1655 (1)	37 (1)
C(222)	5870 (3)	852 (3)	1022 (2)	50 (1)
C(223)	7268 (3)	990 (4)	1084 (2)	68 (1)
C(224)	7649 (3)	1001 (4)	1765 (2)	73 (2)
C(225)	6667 (3)	885 (4)	2392 (2)	70 (1)
C(226)	5269 (3)	761 (3)	2341 (2)	49 (1)
B(1)	−289 (3)	1249 (3)	3627 (2)	44 (1)
B(3)	695 (5)	3207 (3)	2246 (2)	56 (1)
B(2)	554 (4)	2752 (3)	3246 (2)	51 (1)
H(1)	−1202 (29)	1189 (29)	3378 (15)	50 (7)
H(2)	−133 (25)	743 (25)	4173 (13)	30 (6)
H(3)	1177 (34)	3111 (34)	3496 (17)	67 (9)
H(4)	−230 (37)	3147 (36)	1946 (18)	78 (10)
H(5)	1538 (35)	3870 (35)	1977 (17)	68 (9)
H(23)	128 (35)	3721 (36)	2697 (18)	72 (9)
H(12)	−517 (38)	2514 (38)	3658 (19)	80 (10)

[a] Equivalent isotropic U defined as one-third of the trace of the orthogonalized $\mathbf{U}_{ij}$ tensor.

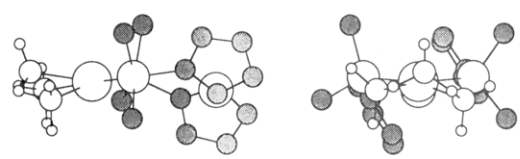

(a) (b)

Figure 3. Detail of the structure of 1 to illustrate the orientation of the B_3H_7 ligand with respect to the PdP_2 unit: (a) viewed along the P---P vector; (b) viewed through the PdP_2 plane. For the phenyl rings, only ipso-C atoms are shown.

Results and Discussion

Molecular Structure of 1. The molecular structure of 1 is illustrated in Figure 2, and bond distances and angles are listed in Table III. The palladium atom in compound 1 acts as a point of fusion for two units of structural interest: (i) the bis(diphenylphosphino)ferrocene

Table III. Selected Bond Distances and Angles for 1 (Labeling Scheme Given in Figure 2)

Bond Distances/Å			
Pd(1)-P(1)	2.366 (1)	Pd(1)-P(2)	2.364 (1)
Pd(1)-B(1)	2.190 (3)	B(1)-B(2)	1.792 (5)
Pd(1)-B(2)	2.154 (3)	B(2)-B(3)	1.787 (5)
Pd(1)-B(3)	2.182 (3)	Fe(1)-C(1)	2.034 (2)
P(1)-C(1)	1.822 (2)	Fe(1)-C(2)	2.035 (3)
P(1)-C(111)	1.833 (2)	Fe(1)-C(3)	2.047 (3)
P(1)-C(121)	1.836 (3)	Fe(1)-C(4)	2.051 (2)
P(2)-C(6)	1.812 (3)	Fe(1)-C(5)	2.049 (2)
P(2)-C(211)	1.841 (2)	Fe(1)-C(6)	2.028 (2)
P(2)-C(221)	1.830 (3)	Fe(1)-C(7)	2.044 (2)
Fe(1)-C(8)	2.055 (3)	Fe(1)-C(9)	2.053 (3)
Fe(1)-C(10)	2.031 (2)	C(1)-C(2)	1.427 (4)
C(2)-C(3)	1.425 (4)	C(3)-C(4)	1.418 (5)
C(4)-C(5)	1.424 (4)	C(1)-C(5)	1.434 (4)
C(6)-C(7)	1.440 (3)	C(7)-C(8)	1.422 (4)
C(8)-C(9)	1.421 (4)	C(9)-C(10)	1.423 (4)
B(1)-H(1)	1.072 (32)	B(1)-H(2)	1.020 (23)
B(3)-H(4)	1.139 (39)	B(3)-H(5)	1.144 (35)
B(2)-H(3)	0.988 (39)	B(1)-H(12)	1.190 (38)
B(5)-H(12)	1.216 (34)	B(3)-H(23)	1.072 (34)
B(2)-H(23)	1.229 (30)		
Bond Angles/deg			
P(2)-Pd(1)-P(1)	104.2 (1)	B(1)-Pd(1)-P(1)	82.6 (1)
B(1)-Pd(1)-P(2)	166.6 (1)	B(3)-Pd(1)-P(1)	168.1 (1)
B(3)-Pd(1)-P(2)	87.4 (1)	B(3)-Pd(1)-B(1)	85.5 (1)
B(2)-Pd(1)P(1)	121.5 (1)	B(2)-Pd(1)-P(2)	130.8 (1)
B(2)-Pd(1)-B(1)	48.7 (1)	B(2)-Pd(1)-B(3)	48.7 (1)
B(3)-B(2)-Pd(1)	66.5 (1)	B(1)-B(2)-Pd(1)	66.7 (1)
B(1)-B(2)-B(3)	112.0 (3)	Pd(1)-B(1)-B(2)	64.6 (1)
B(2)-B(3)-Pd(1)	64.9 (1)	Pd(1)-P(1)-C(1)	119.8 (1)
Pd(1)-P(2)-C(6)	114.4 (1)	B(1)-H(12)-B(2)	96.3 (23)
B(2)-H(23)-B(3)	101.7 (23)	H(4)-B(3)-H(5)	124.1 (22)
H(1)-B(1)-H(2)	120.9 (20)		

chelate and (ii) the triborane ligand derived synthetically from the $[B_3H_8]^-$ anion. The palladium atom in 1 may be described as being in a pseudo-square-planar environment with the phosphorus donors of dppf occupying two of the four sites and the triborane ligand spanning the remaining two. The orientation of the B_3H_7 unit with respect to the PdP_2 plane is illustrated in Figure 3. The borane ligand is twisted through ≈6° with respect to a line joining the two P atoms, but we attribute this small deviation from an otherwise symmetrical disposition to crystal packing forces and regard the borane as being symmetrically bonded to the palladium atom. Figure 1c illustrates that the three B atoms are within bonding distance of the Pd atom, and the Pd–B distances imply that all three palladium–boron interactions are equally important. This feature contrasts sharply with that reported by Guggenberger et al.[2] for the related complex $(Me_2PhP)_2PtB_3H_7$ (Figure 1a) while corroborating the results of Greenwood et al.[3] for the bonding mode of the $\{B_3H_7\}$ fragment in $(OC)(Ph_3P)_2HIrB_3H_7$ (Figure 1b).

The terminal and bridging hydrogen atoms of the borane ligand in 1 have all been directly located (Figure 2) and lie, as expected from a comparison with $(OC)(Ph_3P)_2HIrB_3H_7$,[3] in positions that allow 1 to be considered a formal derivative of *arachno*-B_4H_{10} with the {(dppf)Pd} fragment replacing one $\{BH_3\}$ unit (Figure 4). The internal dihedral angle of the B_4H_{10} butterfly cluster has most recently been reported as 124.5° (by electron diffraction)[17] and 117.4° (by microwave spectroscopy)[18] and these values compare with 129.4° in 1, 126.5° in $(OC)(Ph_3P)_2HIrB_3H_7$,[3] and 127.3° in $(Me_2PhP)_2PtB_3H_7$.[19] On the other hand,

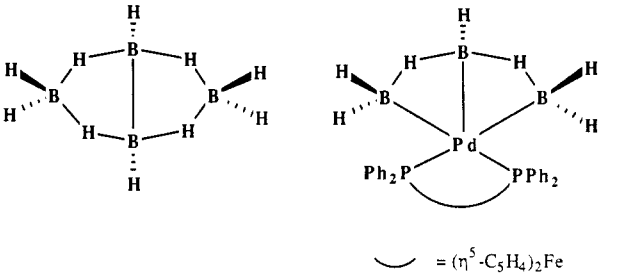

Figure 4. Structural relationship between B_4H_{10} and compound 1.

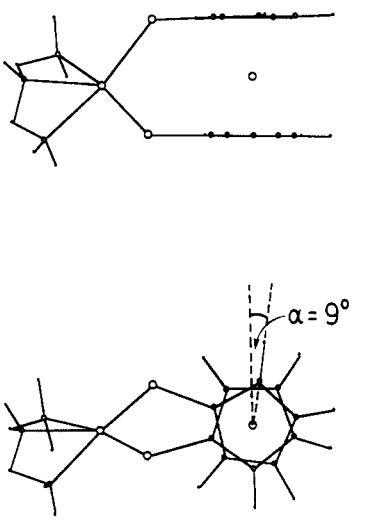

Figure 5. Structure of 1 viewed to illustrate the mutual orientation of the ferrocene rings; Ph substituents are omitted for clarity. The twist angle of 9° measures the deviation from an exactly staggered orientation.

molecular orbital calculations at the extended Hückel level have indicated that the B_3H_7 fragment retains much of its inherent ligand character as it coordinates to a single metal atoms,[5] and in this sense, 1, may be likened to a palladium(II) π-allyl complex. This analogy is examined further in light of ^1H NMR spectroscopic results presented below.

In free dppf, the cyclopentadienyl rings are exactly staggered with a trans arrangement of PPh_2 substituents.[20] Upon chelation, a conformational change is forced upon the ligand,[6,7,21-25] although the final conformation of the two organic rings depends upon the compatibility of the bite angle of dppf and the size of the metal ion. As evidenced via the structural data available for other complexes involving this ligand, dppf has two mechanisms by which to relieve strain, viz., the cyclopentadienyl rings may twist and/or tilt with respect to one another. In 1, the rings are virtually coparallel and are staggered with a twist angle of 9° from an exactly staggered conformation (Figure 5). The staggering necessarily results in the ferrocene unit being skewed with respect to the plane containing the Pd

(17) Dain, C. J.; Downs, A. J.; Laurenson, G. S.; Rankin, D. W. H. *J. Chem. Soc., Dalton Trans.* **1981**, 472.
(18) Simmons, N. P. C.; Burg, A. B.; Beaudet, R. A. *Inorg. Chem.* **1981**, *20*, 533.
(19) The dihedral angle has been calculated by us from crystallographic coordinates in ref 2.
(20) Casellato, U.; Ajo, D.; Valle, G.; Corain, B.; Longato, B.; Grazani, R. *J. Cryst. Spectrosc.* **1988**, *18*, 583.
(21) Onaka, S. *Bull. Chem. Soc. Jpn.* **1986**, *59*, 2359.
(22) Hayashi, T.; Kumada, M.; Higuchi, T.; Hirotsu, K. *J. Organomet. Chem.* **1987**, *334*, 195.
(23) Bruce, M. I.; Butler, I. R.; Cullen, W. R.; Koutsantonis, G. A.; Snow, M. R.; Tiekink, R. T. *Aust. J. Chem.* **1988**, *41*, 963.
(24) Clemente, D. A.; Pilloni, G.; Corain, B.; Longato, B.; Tiripicchio-Camellini, M. *Inorg. Chim. Acta* **1986**, *115*, L9.
(25) Miller, T. M.; Ahmed, K. J.; Wrighton, M. S. *Inorg. Chem.* **1989**, *28*, 2347.

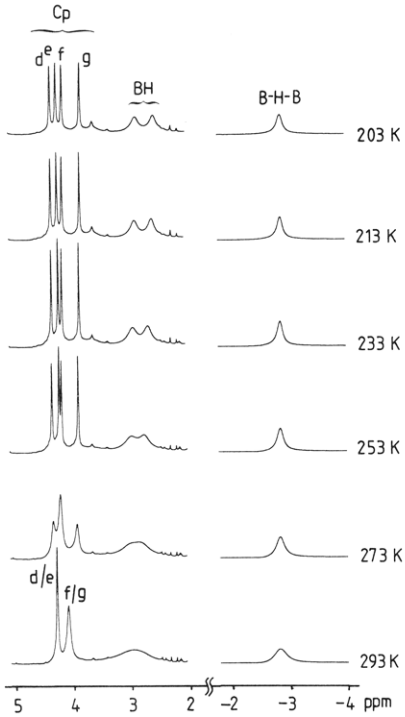

Figure 6. Variable-temperature 400-MHz ^1H NMR spectra for 1 in CD_2Cl_2 solution.

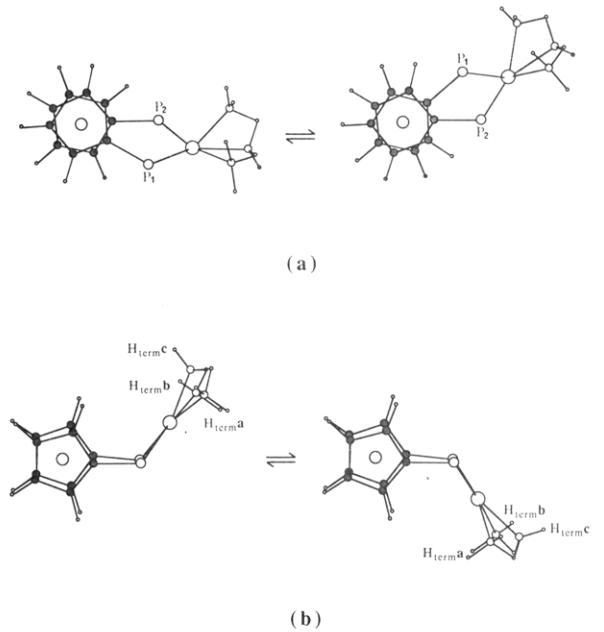

Figure 7. Solution fluxional processes for 1: (a) Cp ring twisting, which averages to give an eclipsed conformation; (b) inversion at the phosphorus atoms, which renders $BH_{term}a$ (i.e., H(1) and H(4) in Figure 2) and $BH_{term}b$ (i.e., H(2) and H(5) in Figure 2) equivalent and provides two environments for $BH_{term}c$ (i.e., H(3) in Figure 2).

and two P atoms, and this is apparent in Figure 3b, in which the ferrocene moiety is positioned behind the $\{P_2PdB_3H_7\}$ unit. The ∠P–Pd–P is 104.2 (1)°, which is slightly larger than has been observed in (dppf)$PdCl_2$[6,7] and the largest angle yet subtended at a metal atom by the dppf ligand.[6,7,21-25] The nonbonded P---P separation in 1 is 3.73 Å, and the Fe---Pd separation is 4.27 Å. It is worth commenting that as a consequence of both the mutual flexibility of the cyclopentadienyl rings and the variation in M–P bond lengths, a large P–M–P bond angle is *not* a prerequisite for a large P---P separation. A comparison of the structural parameters for 1 with those of (dppf)$Mo(CO)_4$ make this point very neatly. The P---P separation in 1 of 3.73 Å is close to that of 3.78 Å in (dppf)$Mo(CO)_4$, and yet the ∠P–Mo–P is only 95.28 (2)° as compared to 104.2 (1)° in 1; this trend is rationalized when one notes that the average Mo–P bond distance is 2.560 (16) Å[7] as compared to a value of Pd–P(av) in 1 of 2.365 (1) Å. In both 1 and (dppf)$Mo(CO)_4$, the cyclopentadienyl rings are staggered (9° and 5.9°, respectively, from a perfectly staggered conformation);[26] in (dppf)$Mo(CO)_4$, the rings deviate 2.2° from coplanarity.

Solution Properties of 1. The ^{11}B NMR spectrum of 1 exhibits unresolved resonances at δ +8.5 (2 B) and +20.1 (1 B) and, apart from a degree of line broadening expected at lower temperatures,[27] these signals are temperature independent. The observed ^{11}B NMR chemical shifts are consistent with a symmetrically bound B_3H_7 fragment, with the terminal boron atoms appearing at higher field than the central atom by virtue of their possessing additional B–H interactions. From Figures 2 and 3, it may be seen that in a static structure of 1, each borane hydrogen atom is unique by virtue of the skewed ferrocene group. Admittedly, the differences in chemical shift between the pairs of protons H(1) and H(4), H(2) and H(5), or H(12) and H(23) would be expected to be small. Contrast this with the situation in $(OC)(Ph_3P)_2HIrB_3H_7$ in which a symmetrical disposition of metal associated ligands means that the B_3H_7 unit gives rise to a 2 (BH_{term}):2 (BH_{term}):1 (BH_{term}):2 (B–H–B) pattern of ^1H NMR signals[4]. The room-temperature ^1H NMR spectrum of 1 exhibits a signal at δ −2.8 assigned to the B–H–B protons and one broad signal centered at δ +2.9, which integrates for all five terminal hydrogen atoms. The results of a variable-temperature ^1H NMR study of compound 1 are illustrated in Figure 6. The signal assigned to the two bridging H atoms sharpens due to ^{11}B–^1H thermal decoupling[28] but does not alter its position, thereby implying static bridges. In contrast, the signal for the BH_{term} hydrogen atoms splits into two peaks at low temperature; one possible explanation for this is, again, simple ^{11}B–^1H thermal decoupling, but the changes in line shape and shift do not appear to be consistent with this reasoning. Furthermore, the spectra in Figure 6 suggest that the process that affects the BH_{term} hydrogen atoms is associated with a mechanism that exchanges the cyclopentadienyl, Cp, protons.

In the static structure of 1, each Cp hydrogen atom is unique (Figure 2), and in solution, such a structure would be characterized by eight signals in the Cp region of the ^1H NMR spectrum. At 203 K, only four resonances (d–g) are observed as shown in Figure 6, and this pattern is consistent with a mutual twisting of the Cp rings, the extent of which is restricted by the fact that dppf is functioning as a bidentate ligand. The net result is that in solution the organic rings appear as though they are eclipsed (Figure 7a). Note that the $\{B_3H_7\}$ unit adopts a position relative to the ferrocene fragment such that the pairs of terminal B–H atoms a (i.e., H(1) and H(4)), and b (i.e., H(2) and H(5)) are distinguishable. In Figure 6, the signals at δ +2.88 and +2.57 observed at 203 K are therefore assigned to B–H_{term}a/b. Atom H(3), BH_{term}c, is unique, but we are unable to detect its resonance at 203

(26) The value of 5.9°, taken from data in ref 7, is defined from an exactly staggered orientation as in Figure 5. The angle given in Figure 2 of ref 7 is 41.9°.

(27) Weiss, R.; Grimes, R. N. *J. Am. Chem. Soc.* **1978**, *100*, 1401.

(28) Beall, H.; Bushweller, C. H. *Chem. Rev.* **1973**, *73*, 465.

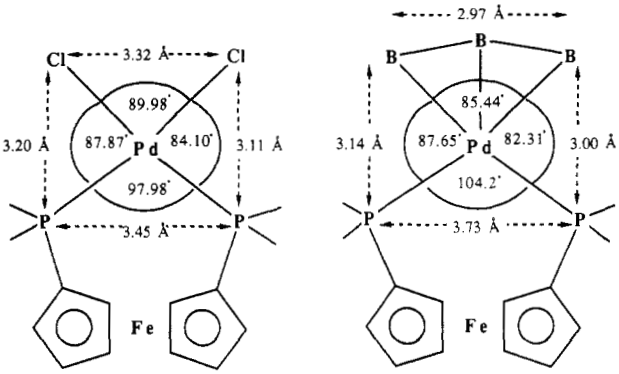

Figure 8. Details of the geometry around the palladium atom in 1 compared to (dppf)$PdCl_2$·CH_2Cl_2.[7]

K. However, results of an ^{11}B–^1H NMR chemical shift correlation experiment have determined that a ^1H NMR resonance for $BH_{term}c$ is hidden under the signals for $BH_{term}a$ and -b. As the temperature is raised to 293 K, the Cp ^1H NMR resonances coalesce as shown in Figure 6 to give two signals (d/e and f/g with assignments confirmed by NOE experiment) that are typical of those expected for the dppf ligand itself. Such average symmetry may be achieved by allowing inversion at each phosphorus atom (Figure 7b). However, the Cp protons are not the only indicator of bridge reversal. As Figure 7b illustrates, inversion at the phosphorus atoms renders $BH_{term}a$ and $BH_{term}b$ essentially equivalent while providing two environments for $BH_{term}c$. Note that $BH_{term}a$ and $BH_{term}b$ cannot be strictly equivalent since the PdB_3 framework is butterfly-shaped rather than planar, and, moreover, the placement of $BH_{term}c$ consistently "labels" one side of the butterfly. In the room temperature ^{11}B–^1H NMR chemical shift correlation spectrum, one cross peak was observed corresponding to a correlation between the terminal protons a and b and the ^{11}B resonance at δ +8.5 (2 B). This implies a single environment for $BH_{term}a$ and $BH_{term}b$. Attempts to observe separate cross peaks for $BH_{term}a$ and $BH_{term}b$ in an ^{11}B–^1H correlation spectrum run at low temperature were inconclusive due to increased line width of the ^{11}B NMR signals.[27] Hence, the broad ^1H NMR resonance at δ +2.9 is an average signal for $BH_{term}a$ and $BH_{term}b$ and also hides the resonances due to $BH_{term}c$.

Reversal barriers in [3]ferrocenophanes containing main-group atom bridges have been examined by Davison[29] and Abel,[30] and the accessibility of an inversion process at arsenic has been illustrated for complexes involving the 1,1′-bis(dimethylarsino)ferrocene chelate.[31,32] For the bulkier dppf ligand, bridge reversal has been proposed and, indeed, appears to be facile in light of data observed on the 400-MHz NMR time scale for the complexes (dppf)-$M(CO)_4$ (M = Mo, Cr); in neither case has a limiting spectrum has been frozen out.[7,33] It is interesting therefore that in 1, as shown in Figure 6, the two fluxional processes (viz. Cp ring twisting and bridge reversal) may be separated, and as expected on purely steric grounds, the energy barrier to inversion at phosphorus is found to be higher than that for mutual ring twisting.

We have compared the fluxional properties of 1 with those of (dppf)$PdCl_2$ (both in dichloromethane solution) and find that the presence of the borane fragment in place of chloride ligands *increases* the barrier to bridge reversal. In the variable-temperature 400-MHz ^1H NMR spectrum of (dppf)$PdCl_2$, resonances at δ +4.42 and +4.22 persist as sharp signals between 293 and 183 K, thereby implying that over this temperature range, Cp ring twisting and inversion at the phosphorus atoms are both thermally accessible processes. For 1, inversion at phosphorus is frozen out at 253 K. The salient features of the geometry around the palladium atom in each compound[34] are presented in Figure 8. Most significantly, although the P–Pd–P bond angle opens up in going from (dppf)-$PdCl_2$·CH_2Cl_2 to 1, the change is counteracted to an extent of ≈73% by the difference in ∠Cl–Pd–Cl and ∠B–Pd–B. The P–Pd–X (X = Cl or B) angle ought to be an important factor in determining the ease with which inversion at the phosphorus atoms may occur. Comparison of the two structures shown in Figure 8 indicates no significant differences in this geometrical parameter. Hence we suggest that it is the inherent rigidity of the borane fragment itself that raises the barrier to phosphorus bridge reversal; in (dppf)$PdCl_2$ deformation of the $PdCl_2$ unit may occur, thereby allowing bridge reversal to occur more readily than in compound 1.

The results of the variable-temperature ^1H NMR spectroscopic studies allow us to comment on one aspect of the analogy drawn previously between the $[B_3H_7]^{2-}$ and π-allyl ligands.[1-5] Fluxional processes involving metal–π-allyls have been well documented.[35] In monomeric (Ph_3P)(π-allyl)PdCl, a system pertinent to a discussion of 1, exchange of terminal hydrogen atoms analogous to a and b in Figure 7 occurs, and the fluxionality may be rationalized in terms of a process involving the formation of a σ-allyl species.[35] Note that in [(π-allyl)$PdCl]_2$, no change in allyl conformation occurs up to 60 °C in $CDCl_3$ solution.[36] In 1, the terminal hydrogen atoms of the borane ligand are certainly rendered equivalent, or approximately equivalent, at ambient temperatures. However, we rule out a mechanism analogous to that experienced by the organic π-allyl ligand for the following reasons. First, rotation about a B–B bond would more than likely involve the bridging hydrogen atom, and Figure 6 illustrates clearly that this is not the case. Second, equivalence of $BH_{term}a$ and $BH_{term}b$ is *not* apparent in systems where inversion at phosphorus is prevented by the geometry of the chelate ring, e.g., in (dppe)PdB_3H_7.[37] Thus, although the term *π-borallyl* may be appropriate with respect to a metal–boron bonding description, the analogy should be regarded cautiously in view of the observed differences in dynamic behavior between Pd(C_3H_5) and Pd(B_3H_7) moieties.

Complexes that incorporate the dppf ligand are expected to exhibit a ferrocene-centered oxidative process. Determining the extent to which this is perturbed by the presence of either a second transition metal or the ligands attached to that metal is of interest since it may provide insight into ways of systematically "tuning" the redox potential of the ferrocene/ferrocenium (Fc/Fc^+) couple. Here, we compare the redox behavior of free dppf, (dppf)$PdCl_2$, and (dppf)PdB_3H_7. In acetonitrile solution, the free dppf ligand is redox active and exhibits a single reversible oxidation in its cyclic voltammogram (+0.51 V

(29) Davison, A.; Smart, J. C. *J. Organomet. Chem.* **1979**, *174*, 321.
(30) Abel, E. W.; Booth, M.; Orrell, K. G. *J. Organomet. Chem.* **1981**, *208*, 213.
(31) Bishop, J. J.; Davison, A. *Inorg. Chem.* **1971**, *10*, 826.
(32) Bishop, J. J.; Davison, A. *Inorg. Chem.* **1971**, *10*, 832.
(33) Note that, due to equivalent ^1H NMR field strengths, results in ref 7 are directly comparable with our own.
(34) Parameters for (dppf)$PdCl_2$·CH_2Cl_2 were used rather than (dppf)$PdCl_2$·$CHCl_3$ since the variable-temperature NMR studies were carried out in CD_2Cl_2 solution.
(35) See for example: Vrieze, K.; Maclean, C.; Cossee, P.; Hilbers, C. W. *C. R. Acad. Sci.* **1966**, *85*, 1077.
(36) Robinson, S. D.; Shaw, B. L. *J. Chem. Soc.* **1964**, 4806.
(37) Haggerty, B. S.; Housecroft, C. E.; Rheingold, A. L.; Shaykh, B. A. M. Submitted for publication.

vs SCE, $E_a - E_c$ = 110 mV, primary reference internal Fc/Fc^+, $E_a - E_c$ = 105 mV). In the complex (dppf)$PdCl_2$, a single reversible oxidation process is also observed (+0.88 V vs SCE, $E_a - E_c$ = 70 mV, primary reference internal Fc/Fc^+, $E_a - E_c$ = 70 mV), which is shifted to a more positive potential with respect to the free ligand. This result is consistent with that reported for (dppf)$PtCl_2$, in which a reversible redox process is similarly observed (≈ +0.90 V vs SCE).[24] A reversible oxidation has also been observed for (dppf)$Re(CO)_3Cl$.[25] In contrast, **1** exhibits a single irreversible anodic wave in its cyclic voltammogram with E_a = +1.0 V vs SCE. The characteristics of this wave are unchanged upon varying the sweep rate (20–200 mV s^{-1}) and temperature (−25 to +25 °C). On the return sweep for **1**, a very broad reduction wave is observed at −0.02 V vs SCE. We have not isolated the product of the irreversible oxidation.

Acknowledgment is made to the Royal Society for a 1983 University Research Fellowship (to C.E.H.), to the Hariri Foundation for a grant (to B.A.M.S.) and to the SERC for a grant (to S.M.O.). We also thank Dr. Edwin C. Constable for assistance with electrochemical measurements.

Supplementary Material Available: Tables of atomic coordinates, bond distances, bond angles, thermal parameters, and H atom coordinates (4 pages); a listing of structure factors (29 pages). Ordering information is given on any current masthead page.

Chemistry of Trivalent Cerium and Uranium Metallocenes: Reactions with Alcohols and Thiols

Stephen D. Stults, Richard A. Andersen,* and Allan Zalkin

Chemistry Department, University of California, and Materials and Chemical Sciences Division, Lawrence Berkeley Laboratory, 1 Cyclotron Road, Berkeley, California 94720

Received November 17, 1989

The trivalent cerium metallocene $(Me_3CC_5H_4)_3Ce$ reacts with alcohols, HOR (R = $CHMe_2$ or Ph), or thiols, HSR (R = $CHMe_2$, or Ph), to give the dimers $(Me_3CC_5H_4)_4Ce_2(\mu\text{-}ER)_2$ as shown by X-ray crystallography for the isopropoxide and isopropylthiolate derivatives. Crystals of $(Me_3CC_5H_4)_4Ce_2(\mu\text{-}OCHMe_2)_2$ are monoclinic, $P2_1/c$ with a = 11.962 (4) Å, b = 14.489 (5) Å, c = 12.384 (5) Å, β = 103.31 (3)°, and V = 2089 Å^3; the structure was refined by full-matrix least-squares methods to a conventional R factor of 0.028, 2874 data, $F^2 > 2\sigma(F^2)$. The Ce_2O_2 unit is planar, the geometry about the cerium atom is pseudotetrahedral, and the geometry is planar about the oxygen atom. Crystals of $(Me_3CC_5H_4)_4Ce_2(\mu\text{-}SCHMe_2)_2$ are also monoclinic, $P2_1/n$ with a = 14.255 (9) Å, b = 13.585 (9) Å, c = 11.265 (7) Å, β = 96.02 (5)°, V = 2170 Å^3; the structure was refined by full-matrix least-squares methods to a conventional R factor of 0.028, 2899 data, $F^2 > 2\sigma(F^2)$. The Ce_2S_2 unit is planar, and the geometry about cerium is pseudotetrahedral though the geometry is pyramidal at sulfur so that the isopropyl groups are anti relative to the Ce_2S_2 ring. Methanol or water give an insoluble solid, presumably $Ce(OMe)_3$ or $Ce(OH)_3$, whereas $HECMe_3$ (E = O or S) do not react with $(Me_3CC_5H_4)_3Ce$, but the thiol does react with the sterically less bulky metallocene $(MeC_5H_4)_3Ce(THF)$ (THF = tetrahydrofuran) to give $(MeC_5H_4)_4Ce_2(\mu\text{-}SCMe_3)_2$. The pK_a's (H_2O) of the organic acids generally predict the thermodynamic outcome of the proton-exchange reactions, though the latter set of experiments show that kinetic (i.e., steric) factors play a role. The uranium metallocene $(Me_3CC_5H_4)_3U$ reacts with HSPh at low temperature to give isolable $(Me_3CC_5H_4)_4U_2(\mu\text{-}SPh)_2$, which rearranges in solution to the monomeric, tetravalent species $(Me_3CC_5H_4)_3USPh$ and unidentified material. The dimer intermediate cannot be detected with the sterically smaller metallocene $(MeC_5H_4)_3U(THF)$, as only $(MeC_5H_4)_3UER$ (ER = OMe, $OCHMe_2$, OPh, and $SCHMe_2$) are isolated.

Binary alkoxide derivatives of the 4f transition metals (lanthanides) traditionally have been prepared by the exchange reaction of a metal halide with either an alkali-metal derivative of an alcohol or an alcohol in ammonia or by reaction of the metal with an alcohol.[1] These synthetic methods are not without difficulties due to halide or oxide contamination as well as formation of anionic compounds.[2] Cyclopentadienylmetal alkoxides have been prepared by metathetical exchange reactions, though difficulties with oxide or halide contamination often makes isolation of pure compounds difficult.[3] A clean synthesis of cyclopentadienyl derivatives such as $(Me_5C_5)_2Lu(OCMe_3)(THF)$ from $(Me_5C_5)_2LuMe_2Li(THF)_2$ and *tert*-butyl alcohol[4a,b] and $(Me_5C_5)_2Yb(OR)$ from $(Me_5C_5)_2Yb$ and diorgano peroxides[4c] are useful when the appropriate starting materials are available. Binary thiolates of the lanthanide elements have not been described,[5] though several cyclopentadienyl derivatives such as $(Me_5C_5)_2Yb(SR)(NH_3)$, prepared from $(Me_5C_5)_2Yb(NH_3)_2$ and R_2S_2, and $(Me_5C_5)_2Lu(SCMe_3)_2Li(THF)_2$, prepared from the thiol and $(Me_5C_5)_2LuMe_2Li(THF)_2$, have been isolated.[4a,b]

* Address correspondence to this author at Chemistry Department, University of California, Berkeley, CA 94720.

(1) (a) Bradley, D. C. *Adv. Inorg. Chem. Radiochem.* **1972**, *15*, 259. (b) Bradley, D. C.; Mehrotra, R. C.; Gaur, D. P. *Metal Alkoxides*; Academic Press: New York, 1978.

(2) (a) Andersen, R. A.; Templeton, D. H.; Zalkin, A. *Inorg. Chem.* **1978**, *17*, 1962. (b) Evans, W. J.; Sollberger, M. S. *Ibid.* **1988**, *27*, 4417. (c) Poncelet, O.; Sartain, W. J.; Hubert-Pfalzgraph; Folting, K.; Caulton, K. G. *Ibid.* **1989**, *28*, 263. (d) Hitchcock, P. B.; Lappert, M. F.; Singh, A. *J. Chem. Soc., Chem. Commun.* **1983**, 1499. (e) Lappert, M. F.; Singh, A.; Atwood, J. L.; Hunter, W. E. *Ibid.* **1981**, 1191.

(3) (a) Evans, W. J.; Sollberger, M. S.; Hanusa, T. P. *J. Am. Chem. Soc.* **1988**, *110*, 1841. (b) Evans, W. J.; Dominguesz, R.; Hanusa, T. P. *Organometallics* **1986**, *5*, 1291.

(4) (a) Schumann, H.; Albrecht, I.; Hahn, E. *Angew. Chem., Int. Ed. Engl.* **1985**, *24*, 985. (b) Schumann, H.; Gallagher, M.; Hahn, E.; Murchmori, C.; Pickardt, J. *J. Organomet. Chem.* **1988**, *349*, 103. (c) Berg, D. J.; Andersen, R. A.; Zalkin, A. *Organometallics* **1988**, *7*, 1858.

(5) Dance, I. G. *Polyhedron* **1986**, *5*, 1037.

0276-7333/90/2309-1623$02.50/0